# Stochastic Elastohydrodynamics of a Microcantilever Oscillating Near a Wall

R. J. Clarke,[1,*] O. E. Jensen,[1,†] J. Billingham,[1] A. P. Pearson,[2] and P. M. Williams[2]

[1]School of Mathematical Sciences, University of Nottingham, Nottingham NG7 2RD, United Kingdom
[2]Laboratory of Biophysics and Surface Analysis, School of Pharmacy, University of Nottingham, Nottingham NG7 2RD, United Kingdom

(Received 9 December 2005; published 8 February 2006)

We consider the thermally driven motion of a microcantilever in a fluid environment near a wall, a configuration characteristic of the atomic force microscope. A theoretical model is presented which accounts for hydrodynamic interactions between the cantilever and wall over a wide range of frequencies and which exploits the fluctuation-dissipation theorem to capture the Brownian dynamics of the coupled fluid-cantilever system. Model predictions are tested against experimental thermal spectra for a cantilever in air and water. The model shows how, in a liquid environment, the effects of non-$\delta$-correlated Brownian forcing appear in the power spectrum, particularly at low frequencies. The model also predicts accurately changes in the spectrum in liquid arising through hydrodynamic wall effects, which we show are strongly mediated by the angle at which the cantilever is tilted relative to the wall.

DOI: 10.1103/PhysRevLett.96.050801 PACS numbers: 07.79.−v, 47.15.−x, 83.10.Mj

Brownian effects in fluids have long been a source of noise contamination in atomic force microscope (AFM) measurements, but techniques have evolved which exploit thermal fluctuations of cantilevers to provide low-amplitude sample measurements [1] and to enable calibration of the cantilever's spring constant [2]. AFM experiments often involve functionalization of the cantilever tip with biological molecules. These molecules require a liquid environment for their native state to be maintained, making it necessary to calibrate the AFM cantilever in liquid. The AFM and other biosensors therefore demand a good understanding of the Brownian dynamics of oscillating microcantilevers in fluid environments.

To address this, Sader [3] extended the analysis of Butt [4], where $\frac{1}{2}k_B\mathcal{T}$ of thermal energy ($k_B$ is Boltzmann's constant and $\mathcal{T}$ temperature) was allocated to each *in vacuo* mode of cantilever oscillation, by incorporating fluid damping in the classical beam equations. Sader's analysis requires that the Brownian forcing is $\delta$ correlated (i.e., has no memory); however, this is valid only if the fluid loading is quasisteady [5,6]. Since an AFM cantilever oscillates in the kHz frequency range, the flows it generates can possess non-negligible unsteady inertia, and the assumption of equipartition of energy among cantilever modes is not justified.

To overcome this difficulty, we follow here an alternative method suggested by Paul and Cross [7] whereby the fluctuation-dissipation theorem is used to predict thermal fluctuations of a cantilever directly from deterministic simulations of the cantilever-fluid dynamics. Our model for the hydrodynamics takes full account of the presence of a nearby wall [8,9], and demonstrates the striking sensitivity of spectra to the angle at which the cantilever is tilted relative to the wall (a configuration difficult to model using Sader's method). We present new experimental results against which we test our analysis.

We consider a rectangular cantilever of length $L$, width $D = \epsilon L$ ($\ll L$), and thickness $B$ ($\ll D$), at a height $H(x)$ above a plane horizontal wall, where $x$ measures distance along the long axis of the cantilever from its clamped end. The cantilever is tilted at a small angle $\alpha$ to the horizontal, such that $\mathcal{H} \equiv H(L)$ is the minimum height from the wall. The cantilever has Young's modulus $E$, moment of inertia $I$, density $\rho_c$, and mass per unit length $m_c = \rho_c BD$. It is immersed in fluid of viscosity $\nu$ and density $\rho$. Oscillations of the cantilever take place in a vertical plane and are assumed to be of amplitude comparable to the thermal scale $A \equiv \sqrt{k_B\mathcal{T}L^3/EI}$. Assuming $A \ll B$, we can model the motion using a linear Euler-Bernoulli beam equation and the fluid flow with the linearized unsteady Stokes equations. At its unclamped end, the beam is assumed to be subject to a point torque $(k_B\mathcal{T}L/A)T(t)$ at time $t$. Writing $x = L\xi$ and frequency $\omega^* = \omega_0\omega$, where $\omega_0 \equiv \sqrt{EI/m_cL^4}$, transverse displacements $Aw(\xi, t)$ in the temporal Fourier domain $A\hat{w}(\xi, \omega)$ satisfy the dimensionless beam equation [3]

$$\hat{w}_{\xi\xi\xi\xi} = \kappa^4\hat{w} \qquad (0 \le \xi \le 1) \tag{1}$$

(ignoring stochastic forcing for the present), subject to $\hat{w} = \hat{w}_\xi = 0$ at $\xi = 0$ and $\hat{w}_{\xi\xi} = \hat{T}(\omega)$, $\hat{w}_{\xi\xi\xi} = 0$ at $\xi = 1$. Here

$$\kappa \equiv [\omega^2 + i\omega M\Omega\Gamma(\gamma, H/L)]^{1/4}, \tag{2}$$

$$\gamma \equiv \epsilon M^{-1/2}\omega^{1/2} = D(\omega^*/\nu)^{1/2}, \tag{3}$$

where $M \equiv \nu/\omega_0L^2$ relates fluid loading to bending forces and $\Omega \equiv L^2\rho/m_c$ is the fluid/beam density ratio. The $\omega^2$ term in (2) represents beam inertia and the $\Gamma$ term is the hydrodynamic drag per unit length, accounting both for viscous and unsteady inertial forces in the fluid. We assume

 

that the induced flow is locally two-dimensional, so that $\Gamma$ depends only on the local distance between the cantilever and wall $H(x)/L$ and the frequency parameter $\gamma$ [see (3)], which relates the cantilever width to the thickness of viscous boundary (or Stokes) layers. The validity of the locally two-dimensional assumption is justified (for an oscillating rigid cylinder) when two independent screening effects are effective, one arising at high frequencies (for $\gamma \gg \epsilon$) and the other at low cantilever-wall separation and low tilt angle (for $\mathcal{H} \ll L$, $\alpha \ll 1$) [9]; however, three-dimensional flows are significant for high-order modes of a flexible cantilever [10]. The drag $\Gamma$ is determined using boundary-integral computations for a rectangular cylinder oscillating normally to a wall [8] (see also Ref. [11]); thus, in general (for $\alpha \neq 0$), $\Gamma$ varies along the length of the cantilever. For a cantilever far from a wall, Stokes' expression for the drag on an oscillating circular cylinder of width $D$,

$$\Gamma_S = i\pi\gamma^2\{1 + 4K_1(\sqrt{i}\gamma)/[\sqrt{i}\gamma K_0(\sqrt{i}\gamma)]\}, \quad (4)$$

where $K_0$ and $K_1$ are modified Bessel functions, provides an effective approximation [3]. We assume no slip at the cantilever surface, a reasonable assumption in most liquid environments [8].

We characterize the cantilever's motion by the angle of deflection at the tip, $\hat{W}_\xi(\omega) \equiv \hat{w}_\xi(1, \omega)$, under various torques. Setting $T(t) = \delta(t)$ for example, so that $\hat{w}_{\xi\xi} = 1$ at $\xi = 1$, $\hat{W}_\xi$ gives the system's dynamic susceptibility $\chi(\omega) \equiv \hat{w}_\xi(1, \omega)$. In general, we determine this numerically, by solving the damped cantilever dynamics (1) plus boundary conditions using a finite difference method, where $\Gamma$ is computed numerically at each discretization point [8]. For nontilted cantilevers with $\mathcal{H} \gg L$, it is straightforward to show that

$$\chi(\omega) = \frac{\cos\kappa \sinh\kappa + \sin\kappa \cosh\kappa}{\kappa(1 + \cos\kappa \cosh\kappa)}, \quad (5)$$

where $\kappa$ is given by (2) and $\Gamma$ by $\Gamma_S$ . The response to a general torque $T(t)$ is then $\hat{W}_\xi(\omega) = \chi(\omega)\hat{T}(\omega)$.

We use the fluctuation-dissipation theorem to obtain the thermal power spectrum of the cantilever tip's angle of deflection under Brownian forcing, following Ref. [7]. Equilibrium fluctuations of the cantilever are probed by placing the cantilever into a nonequilibrium state through application of a small torque to its tip, so that $T(t) = T_0$ for $t < 0$ and $T(t) = 0$ for $t > 0$, so that

$$\hat{T}(\omega) = T_0[\pi\delta(\omega) + i/\omega]. \quad (6)$$

As the cantilever tip decays back to equilibrium, the average value for its tip deflection $\langle W_\xi(t)\rangle_{\text{neq}}$ satisfies [12]

$$\langle W_\xi(t)\rangle_{\text{neq}} = T_0 C(t), \quad (7)$$

where $C(t) \equiv \langle W_\xi(t) W_\xi(0)\rangle_{\text{eq}}$ measures the correlation between initial fluctuations of the tip deflection about the equilibrium location and those at time $t > 0$. The connection between the laws governing the microscopic and macroscopic dates back to the regression hypothesis of Onsager [13], which states that the regression of spontaneous microscopic fluctuations in an equilibrium system are governed by the same laws that describe the relaxation of macroscopic nonequilibrium disturbances. These macroscopic disturbances are represented simply by the averaged microscopic state $\langle W_\xi(t)\rangle_{\text{neq}}$. This is determined knowing the susceptibility of the system using

$$\langle \hat{W}_\xi(\omega)\rangle_{\text{neq}} = \chi(\omega)\hat{T}(\omega) \quad (8)$$

with $\hat{T}$ given by (6). Combining (7) and (8) gives

$$C(t) = \frac{1}{2\pi T_0}\int_{-\infty}^{\infty} \chi(\omega)\hat{T}(\omega)e^{i\omega t}d\omega = \frac{-1}{\pi}\int_{-\infty}^{\infty} \frac{\chi(\omega)}{\omega}\sin\omega t d\omega. \quad (9)$$

In computing $C(t)$ when $\alpha = 0$ and $\mathcal{H} \gg L$ by contour integration [using (2)–(5)], there are contributions from poles $\omega = \omega_k$ in $\text{Im}(\omega) > 0$ satisfying $1 + \cos\kappa \cosh\kappa = 0$, which capture the behavior of the *in vacuo* modes damped by the presence of the fluid. Because $\kappa$ depends on $\sqrt{\omega}$ via $\gamma$ [see (2) and (3)], $\chi(\omega)$ also has a branch cut along $\text{Im}(\omega) > 0$ which captures the continuous spectrum of disturbances that leads to the algebraic decay of $C(t)$ as $t \to \infty$, associated with the fact that the Brownian forcing is not $\delta$ correlated.

The power spectrum of the tip's deflection angle $[P^*(\omega^*) = (A^2/\omega_0)P(\omega)]$ is found in dimensionless form by taking the Fourier cosine transform of (9),

$$P(\omega) \equiv 2\int_0^{\infty} C(t)\cos\omega t dt = -\frac{2}{\pi}\int_{-\infty}^{\infty} \frac{\chi(\omega')}{\omega'^2 - \omega^2}d\omega' = 2\frac{\Im[\chi(\omega)]}{\omega} \quad (10)$$

by the residue theorem (see also Ref. [14]). The thermal spectrum is therefore given in terms of the susceptibility $\chi$, which can be computed deterministically. When $\Gamma = \Gamma_S$ [see (4)], it is instructive to decompose (10) into contributions from the discrete and continuous components of the autocorrelation function. The residue theorem yields

$$P(\omega) = \int_0^{\infty} \frac{-\text{Im}[\chi(i\sqrt{x})]}{\pi(x^2 + \omega^2)}dx - 2i\sum_{k=1}^{\infty} \frac{\Lambda_k/(\kappa_k\kappa_k')}{\omega_k^2 - \omega^2}, \quad (11)$$

$$\Lambda_k = \frac{\cos\kappa_k \sinh\kappa_k + \sin\kappa_k \cosh\kappa_k}{\cos\kappa_k \sinh\kappa_k - \sin\kappa_k \cosh\kappa_k}, \quad (12)$$

$$\kappa_k' = \frac{\kappa_k}{2\omega_k}\left(\frac{K_0^2 + 2M\lambda_k^{-1}K_1K_0 + MK_1^2}{K_0^2 + 4M\lambda_k^{-1}K_0K_1 + MK_0^2}\right), \quad (13)$$

where $\kappa(\omega)$ evaluated near $\omega_k$ is written $\kappa = \kappa_k + \kappa_k'(\omega - \omega_k) + \cdots$, and $\lambda_k \equiv \sqrt{i}\gamma_k$ is evaluated at $\omega = \omega_k$, as are $K_0(\lambda_k)$, $K_1(\lambda_k)$ in (13). The branch cut, which has its origins in the unsteady diffusion of vorticity from the cantilever surface into the fluid, produces an integral contribution to the power spectrum in (11).

Experiments were conducted using a molecular force probe (MFP-1D) (Asylum Research, Santa Barbara, CA) and a rectangular silicon nitride cantilever (MLCT microlever, cantilever B, Veeco) coated with gold on the back surface and with a pyramidal tip, about 2 $\mu$m high, on the opposite surface. The same cantilever was used to collect thermal spectra in air and in water. The water used was Ultrapure, with a resistance of 18.2 M$\Omega$ cm, and was passed through a 0.2 $\mu$m filter prior to use. Freshly cleaved mica was used as the substrate and all measurements - were conducted at room temperature. High-resolution measurements of the cantilever's dimensions were obtained using scanning-electron microscopy which showed that $(L, D, B) = (232.4, 20.11, 0.573)$ $\mu$m. Raw deflection data, representing the thermal noise of the cantilever, were collected over 10 s and processed using Asylum Research software (IGOR Pro, Wavemetrics) to generate thermal power spectra. We present experimental spectra (square-rooted) obtained in air (Fig. 1) and water when far from and nearby the solid substrate (Figs. 2 and 3 respectively).

By gold-coating the cantilever to improve its reflectivity, we altered its material properties, making it necessary to determine the effective density $\rho_c$ by fitting theoretical predictions to the thermal spectrum; this was done in air, where the resonant peaks are well defined. Varying $\rho_c$ in the theoretical model changes the height-to-width ratio (quality factor) of the first resonant peak; $\rho_c = 5.3$ g cm$^{-3}$ gave the best fit (in approximate agreement with similar experiments by Chon *et al.* [15]), both for Sader's model [3] and using (10). We then normalized the theoretical spectra so that the amplitude of the first resonant peak in air matched its experimental value. These values for the density and normalization constant were then used for predicting spectra in water (Figs. 2 and 3). Neither theoretical model accounts for $1/\omega^*$ noise at low frequencies (evident in Fig. 1) due to mechanical vibrations from the apparatus, or for low-level white noise from the apparatus electronics giving a nonzero spectral baseline. Neither model captures the second harmonic exactly (Fig. 1), with discrepancies between theory and experiment possibly arising from a number of different factors, including three-dimensional flows along the cantilever's axis [10], hydrodynamic interactions with other cantilevers attached to the same support and torsional motion [16].

In water (Fig. 2) both theoretical models work well in capturing the shift in location, amplitude, and sharpness of the resonant peaks as the density of the surrounding medium is increased. However, the fluctuation-dissipation approach (10) offers noticeable improvements over Sader's method. At low frequencies, in particular (see the inset), the two predictions diverge significantly. This can be attributed in part to the neglect by Sader's method of memory effects in the fluid motion: neglecting the continuous component of the power spectrum [the integral in (11), representing Brownian forcing that is not $\delta$ correlated], leads to a noticeable overestimate of the height of the spectrum for $\omega^* \leq 2$ kHz (Fig. 2, inset). We attribute the divergence between the experimental spectrum and the fluctuation-dissipation prediction below 1 KHz to $1/\omega^*$ noise.

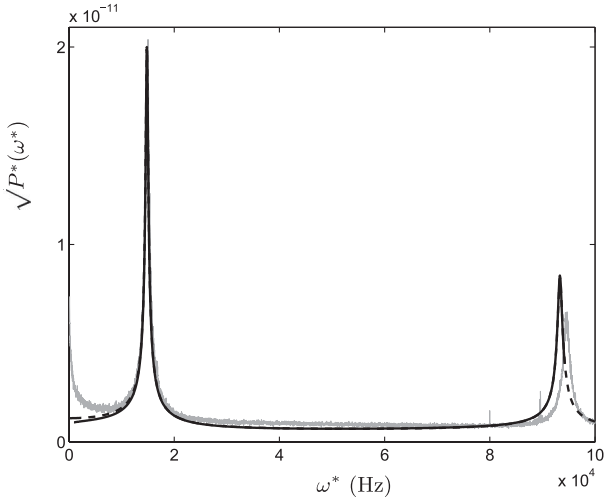


FIG. 1. Thermal power spectrum of the cantilever tip's angle of deflection, measured in air far from the substrate, showing experiment (gray, solid line), predictions using Sader's method [3] (black, dashed line) and Eqs. (4), (5), and (10) (black, solid line).

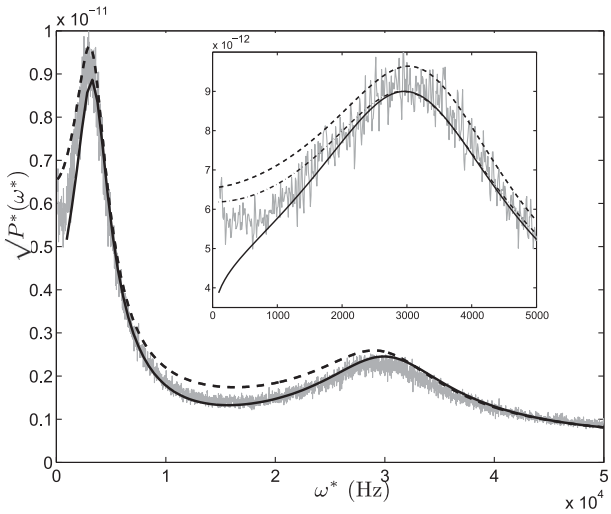


FIG. 2. Thermal power spectrum, measured in water far from the substrate, showing experiment (gray, solid line), predictions using Sader's method [3] (black, dashed line) and Eqs. (4), (5), and (10) (black, solid line). Inset: a close-up of the first harmonic, where, in addition, the dash-dotted line gives the power spectrum computed without the inclusion of the branch-cut integral in (11).

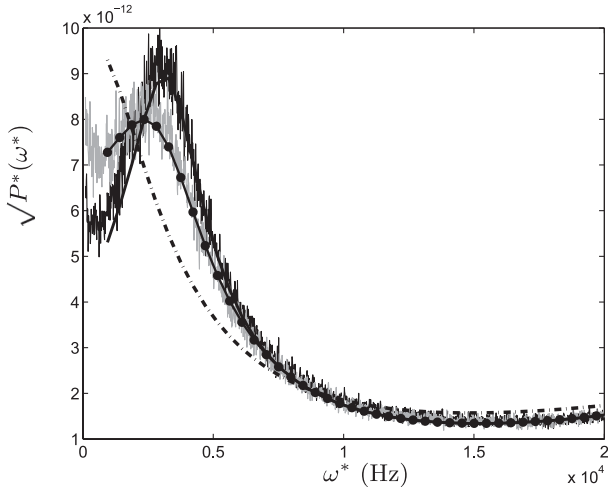


FIG. 3. Thermal power spectrum in water near a wall. Experimental data for a cantilever tilted at $\pi/12$ to the wall are shown at minimum separation $\mathcal{H} = 70$ $\mu$m (solid black line, higher peak) and $\mathcal{H} = 8.87$ $\mu$m (solid gray line, lower peak). Theoretical predictions using (10) are shown for $\mathcal{H} = 70$ $\mu$m (solid line); $\mathcal{H} = 8.87$ $\mu$m, $\alpha = \pi/12$ (solid line with dots); $\mathcal{H} = 8.87$ $\mu$m, $\alpha = 0$ (dash-dotted line).

Figure 3 shows how, when the cantilever is moved close to the substrate, wall effects produce a shift in the spectrum which is captured well by (10). The thermal spectrum obtained experimentally, at a minimum separation distance $\mathcal{H} = 8.87$ $\mu$m, has a lower amplitude, resonant frequency, and quality factor than at $\mathcal{H} = 70$ $\mu$m, where wall effects are weaker. These changes are captured well by (10) when the hydrodynamic drag is computed using a two-dimensional boundary-element method for a rectangular cantilever near a wall [8], accounting for tilt of $\alpha = \pi/12$ through varying the ratio $H(x)/L$ in (2). If tilt is ignored, the hydrodynamic loading on the cantilever is artificially high and the predicted spectrum is substantially altered, no longer displaying a well defined peak (Fig. 3, $\alpha = 0$).

In conclusion, we have demonstrated the effectiveness of an approach exploiting the fluctuation-dissipation theorem [7] for describing the Brownian dynamics of an AFM cantilever and we have highlighted differences with the popular model due to Sader [3]. In gases, both approaches give near-identical spectra (Fig. 1), although each overpredicts the amplitude of the second harmonic; this warrants further investigation. In water, however, the fluctuation-dissipation approach gives a more accurate prediction of the shape of the first and second resonant peaks, and the effects of the long-time tail in the autocorrelation appears in the power spectrum at low frequencies. Furthermore, in the presence of hydrodynamic wall effects, the fluctuation-dissipation approach, supplemented with accurate predictions of drag that vary along the length of the tilted cantilever [8], captures accurately the shift in amplitude and resonant frequency observed in the experimental data. These results have important consequences for experimentalists wishing to extract properties of the cantilever and the sample through parameter fitting using thermal methods [1].

This work was supported by EPSRC Grant No. GR/R88991/01. Comments from Professor Michael Cross and Professor Xingyong Chen are gratefully acknowledged.

*Present address: School of Mathematical Sciences, University of Adelaide, Adelaide, SA 5005, Australia.
†Electronic address: Oliver.Jensen@nottingham.ac.uk

[1] R. Rajagopalan, Colloids Surf. A **174**, 253 (2000).
[2] J. L. Hutter and J. Bechhoefer, Rev. Sci. Instrum. **64**, 1868 (1993).
[3] J. E. Sader, J. Appl. Phys. **84**, 64 (1998).
[4] H.-J. Butt and M. Jaschke, Nanotechnology **6**, 1 (1995).
[5] R. Zwanzig and M. Bixon, Phys. Rev. A **2**, 2005 (1970).
[6] E. J. Hinch, J. Fluid Mech. **72**, 499 (1975).
[7] M. R. Paul and M. C. Cross, Phys. Rev. Lett. **92**, 235501 (2004).
[8] R. J. Clarke, S. M. Cox, P. M. Williams, and O. E. Jensen, J. Fluid Mech. **545**, 397 (2005).
[9] R. J. Clarke, O. E. Jensen, J. Billingham, and P. M. Williams, Proc. R. Soc. A **462**, 913 (2006).
[10] A. Maali, C. Hurth, R. Boisgard, C. Jai, T. Cohen-Bouhacina, and J. P. Aime, J. Appl. Phys. **97**, 074907 (2005).
[11] C. P. Green and J. E. Sader, Phys. Fluids **17**, 073102 (2005).
[12] D. Chandler, *Introduction to Modern Statistical Physics* (Oxford University Press, New York, 1987).
[13] L. Onsager, Phys. Rev. **37**, 405 (1931).
[14] H. Ma, J. Jimenez, and R. Rajagopalan, Langmuir **16**, 2254 (2000).
[15] J. W. M. Chon, P. Mulvaney, and J. E. Sader, J. Appl. Phys. **87**, 3978 (2000).
[16] J. E. Sader and C. P. Green, J. Appl. Phys. **92**, 6262 (2002).